Electrosyntheses and Characterizations of a New Multielectrochromic Copolymer of 1-(3-methylthiophen-2-yl)pyrene and 3,4-ethylenedioxythiophene

Guoqiang Feng[1], Zhong Wang[2], Qingxin Gao[3], Shuang Chen[3,], Xiaolong Xu[3]*

[1]School of Petroleum Engineering, China University of Petroleum (East China), QingDao, 266580, P. R. China
[2] The Liaocheng Hospital, Liaocheng, Shandong, 252000, P.R. China
[3] College of Chemical Engineering, China University of Petroleum (East China), QingDao, 266580, P. R. China
*E-mail: chsh1030@163.com

1-(3-Methylthiophen-2-yl)pyrene (MTP) monomer was successfully synthesized via coupling reaction. A novel conjugated copolymer based on 1-(3-methylthiophen-2-yl)pyrene (MTP) and 3,4-ethylenedioxythiophene (EDOT) was electrochemically synthesized and characterized. Characterizations of the resulting copolymer P(MTP-co-EDOT) were performed by cyclic voltammetry (CV), UV-vis spectroscopy and scanning electron microscopy (SEM). Compared with the MTP and the EDOT homopolymers, P(MTP-co-EDOT) film had distinct electrochromic properties via spectroelectrochemical analysis, and it exhibited four different colors (purple, brown, grass green and dusty blue) under various potentials. Moreover, the copolymer film showed high optical contrasts and satisfactory response times. An electrochromic device (ECD) based on P(MTP-co-EDOT) and poly(3,4-ethylenedioxythiophene) (PEDOT) was constructed and characterized. The ECD was found to have a high optical contrast, fast response time, satisfactory optical memories and good redox stability.

1. INTRODUCTION

Electrochromism is defined as a character in some materials which enable them to electrochemically switch between different colored states as a result of redox reactions under an applied electric field [1]. The synthesis of novel electrochromic materials is always a considerable

research direction. Over the past decades, electrochromic materials have been extensively studied in various application fields, such as polymer solar cells, sensors, smart windows, electrochromic devices (ECDs) and so on [2-5]. Among them, conjugated polymers have attracted the attention of scientists owing to excellent performance, rational use of energy and environmentally friendly. For conjugated polymers, the electrochromism is related to doping-dedoping process. The doping process modifies the polymer electronic structure, producing new electronic states in the band gap and causing color changes. Electronic absorption shifts bathochromically upon doping, and the color contrast between the dedoped and doped states is related to the polymer band gap [6].

Recently, pyrene and its derivatives are more attractive to us because of their fluorescent properties, and they have several advantages over other compounds, such as high quantum efficiency, carrier mobility, and hole-transporting ability [7]. Thiophene-based materials, as a series of functional materials, have gained much attention during the past decades. Moreover, it has been known that the introduction of aromatic bridge in the bithiophenic polymer main chains could result in changed HOMO-LUMO band gap polymers compared with both homopolymers [8]. We wish to synthesis a novel polymer involved a combination of a pyrene unit and a 3-methylthiophene unit.
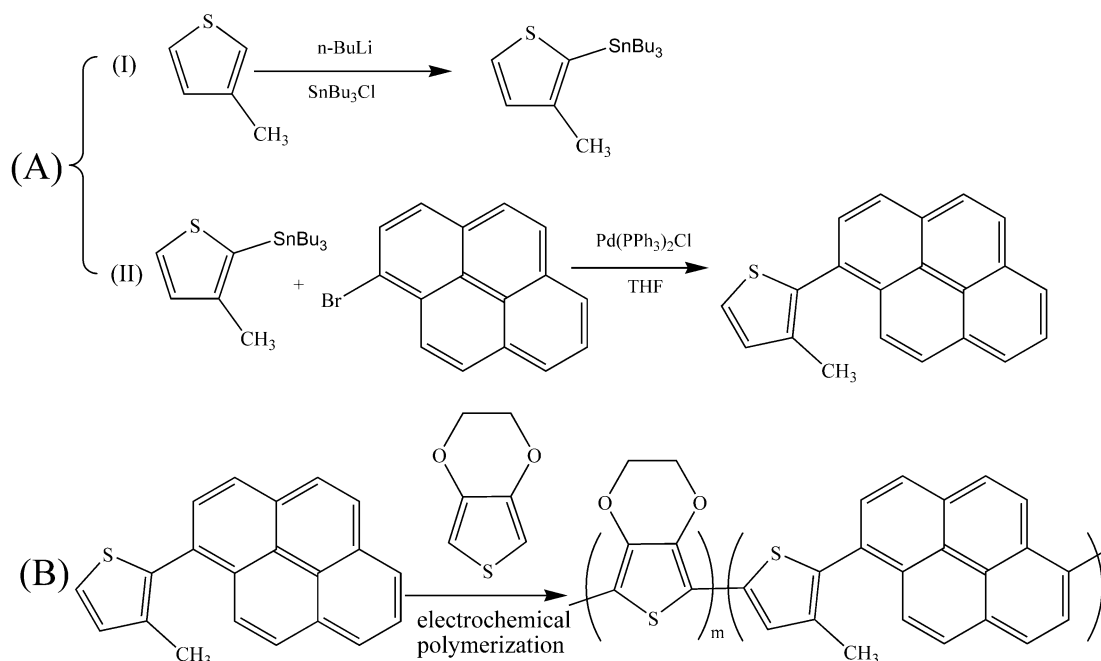
Scheme 1. Synthetic routes of (A) MTP and (B) copolymer of MTP and EDOT.

Meanwhile, fine tuning in the band gap can be achieved by tailoring the co-monomer feed ratio of copolymerization [9]. 3, 4-Ethylenedioxythiophene (EDOT) is a sensible choice as a co-monomer since it produces a low band gap polymer with high stability and good conductivity [10]. And 3, 4-ethylenedioxythiophene (EDOT) has recently exhibited superior stability of conductivity [11]. It gives rise to noncovalent intramolecular interactions with adjacent thiophenic units and thus actuates self-rigidification of the π-conjugated system in which it is incorporated [12]. Recently, to modify the properties of PEDOT, lots of research works have been focused on the electro-chemical

copolymerization of ethylenedioxythiophene (EDOT) with pyrrole, thiophene, and its derivatives [13, 14].

According to above considerations, in this work, we synthesized the monomer of 1-(3-methylthiophen-2-yl)pyrene (MTP) via coupling reaction (Scheme 1(A)) by our group. Then we synthesized the copolymer via the electrochemical oxidation of MTP/EDOT mixtures in ACN solution containing 0.2 M NaClO$_4$ as a supporting electrolyte (Scheme 1(B)). The copolymer film revealed four different colors (purple, brown, grass green and dusty blue). To explore the use of this material in electrochromic device we constructed a dual-type electrochromic device with ITO/copolymer/gel electrolyte/PEDOT/ITO configuration, where the copolymer and PEDOT functioned as the anodically and the cathodically coloring layers respectively. Characterizations of the electrochromic behavior of the copolymer and the electrochromic device were achieved by spectroelectrochemistry, kinetic, colorimetry studies.

2. EXPERIMENTAL

2.1. Materials

1-(3-Methylthiophen-2-yl)pyrene (MTP) monomer was synthesized by our group, 3,4-ethylenedioxythiophene (EDOT, 98%). Commercial high-performance liquid chromatography grade acetonitrile (ACN, Tedia Company, INC., USA), poly(methyl methacrylate) (PMMA, Shanghai Chemical Reagent Company), propylene carbonate (PC, Shanghai Chemical Reagent Company) and lithium perchlorate (LiClO$_4$, Shanghai Chemical Reagent Company, 99.9%) were used directly without further purification. Sodium perchlorate (NaClO$_4$, Shanghai Chemical Reagent Company, 98%) was dried in a vacuum at 60 ºC for 24 h before use. Other reagents were all used as received without further treatment. Indium-tin-oxide-coated (ITO) glass (sheet resistance : < 10 Ω □$^{-1}$, purchased from Shenzhen CSG Display Technologies, China) was washed with ethanol, acetone and deionized water successively under ultrasonic, and then dried by N$_2$ flow.

2.2. Instrumentation

^{1}H NMR spectroscopy studies were carried out on a Varian AMX 400 spectrometer and tetramethylsilane (TMS) was used as the internal standard for ^{1}H NMR. Scanning electron microscopy (SEM) measurements were taken by using a Hitachi SU-70 thermionic field emission SEM. UV-vis spectra were carried out on a Perkin-Elmer Lambda 900 UV-vis-near-infrared spectrophotometer. Digital photographs of the polymer films and electrochromic devices were taken by a Canon Power Shot A3000 IS digital camera.

2.3. Electrochemistry

Electrochemical syntheses and experiments were performed in an one-compartment cell with a CHI 760 C Electrochemical Analyzer (Shanghai ChenHua Instrument Co. China) under control of a

computer. The working electrodes was a platinum wire with a diameter of 0.5mm, a platinum ring worked as counter electrode, and a silver wire (Ag wire) was taken as pseudo reference electrode. The working and counter electrodes for cyclic voltammetric experiments were placed 0.5cm apart during the experiments. All electrochemical polymerization and CV tests were taken in ACN solution containing 0.2 M NaClO$_4$ as a supporting electrolyte. The pseudo reference electrode was calibrated externally using a 5 mM solution of ferrocene (Fc/Fc$^+$) in the electrolyte (E$_{1/2}$(Fc/Fc$^+$) = 0.20 V vs. Ag wire in ACN solution containing 0.2 M NaClO$_4$). All the potentials mentioned were vs. the Ag wire electrode. The half-wave potential (E$_{1/2}$) of Fc/Fc$^+$ measured in 0.2 M NaClO4/ACN solution was 0.28 V vs. SCE. Thus, the potential of Ag wire was assumed to be 0.08 V vs. SCE [8]. All of the electrochemical experiments were carried out at room temperature under nitrogen atmosphere. The amount of polymers deposited on a platinum electrode was controlled by the integrated charge passed through the cell for electrochemical tests. Cyclic voltammetry (CV) of the polymer was carried out with the same electrode set-up in monomer-free electrolyte solution.

2.4. Preparation for measurements

To obtain sufficient amount of polymers for spectra analysis and SEM measurements, a three-electrode cell assembly was used where the working electrode was an ITO glass with a surface area of 0.9×2.0 cm^2, the counter electrode was a stainless steel wire, and an Ag wire was used as pseudo-reference electrode. The copolymer films for spectroelectrochemistry were prepared by potentiostatically deposition on ITO electrode. After electrochemical polymerization, electrochemical dedoping was carried out in ACN solution containing 0.2 M NaClO$_4$ for 30 minutes. Then the copolymer was washed with ACN for 3 times to remove the supporting electrolyte and oligomers/monomers.

2.5. Preparation of the gel electrolyte

A gel electrolyte based on PMMA and LiClO$_4$ was plasticized with PC to form a highly transparent and conductive gel. ACN was also included as a high vapor pressure solvent to allow an easy mixing of the gel components. The composition of the casting solution by weight ratio of ACN:PC:PMMA:LiClO$_4$ was 70:20:7:3. The gel electrolyte was used for construction of the polymer cell [15].

2.6. Construction of electrochromic devices

Electrochromic devices (ECDs) were constructed using two complementary polymers, namely P(MTP-co-EDOT) as the anodic material and PEDOT as the cathodic material. Both P(MTP-co-EDOT) and PEDOT films were electrodeposited on two ITO glasses (the active area: 1.8 cm × 2.0 cm) at 1.4 V. Electrochromic device was built by arranging the two polymer films (one oxidized, the other reduced) facing each other separated by a gel electrolyte.

3. RESULTS AND DISCUSSION

3.1. Electrochemical polymerization and characterization of polymers

3.1.1. Electrochemical polymerization

The anodic polarization curves of 0.005 M MTP, 0.005 M EDOT and the MTP/EDOT mixture at 1:1 in ACN solution containing 0.2 M NaClO$_4$ are showed in Fig. 1. The onset oxidation potential (E_{onset}) of MTP in the solution is 1.31 V (Fig. 1a), while that of EDOT is 1.17 V (Fig. 1c). It is well known that successful electrochemical copolymerization of different monomers is due to the fact that the E_{onset} of the monomers are close to each other [16, 17]. The difference of the onset oxidation potential between MTP and EDOT is 0.14 V, implying that the electrochemical copolymerization is readily to be achieved [18, 19]. As can been seen from Fig. 1b, the E_{onset} of the P(MTP-co-EDOT) is 1.39 V, which is higher than those of MTP and EDOT, indicating the existence of the interaction between two monomers in 0.2 M NaClO$_4$/ACN solution [20]. The synthetic route of the copolymer of MTP and EDOT is illustrated in Scheme 1.
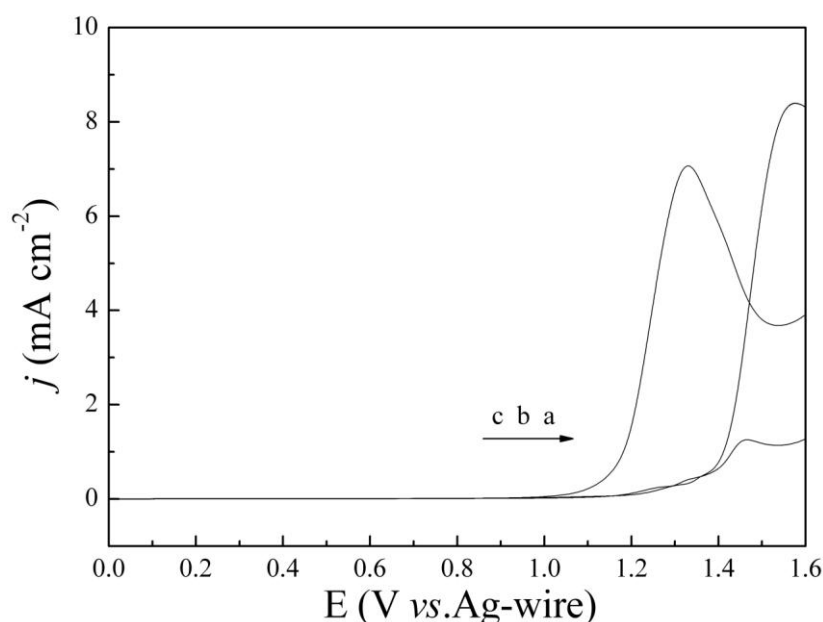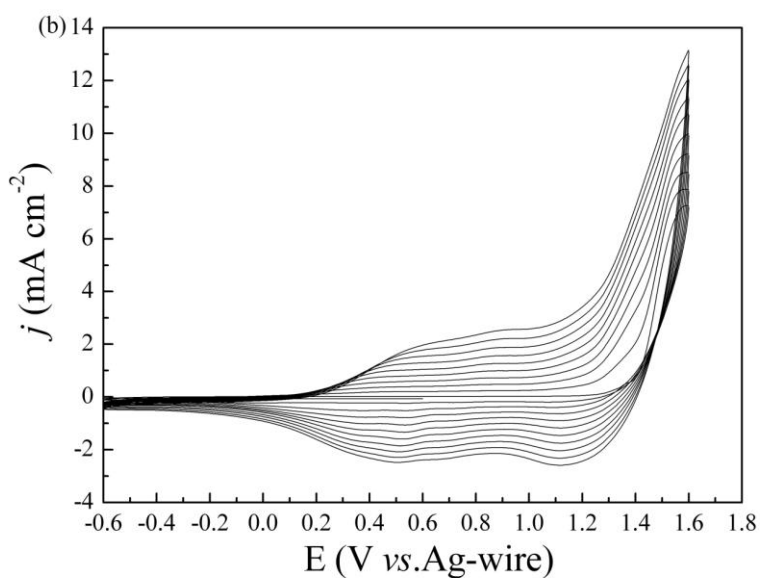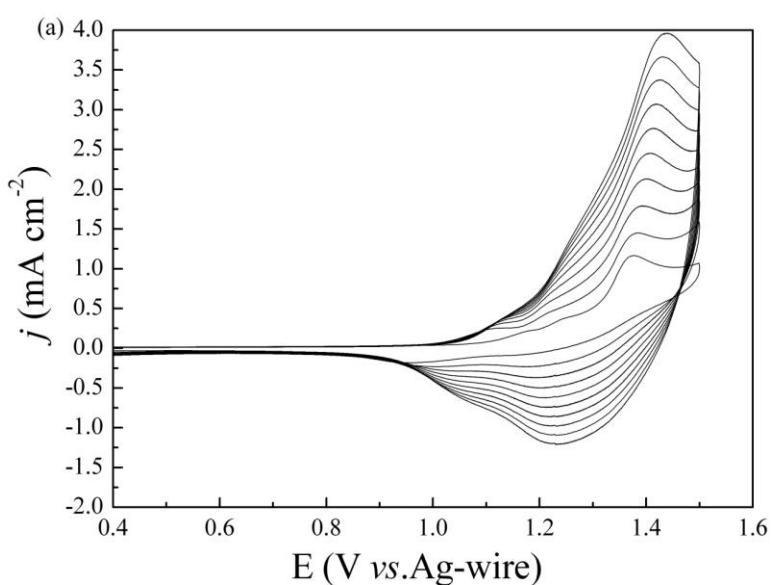

Figure 1. Anodic polarization curves of (a) 0.005 M MTP, (b) the mixture of 0.005 M MTP and 0.005 EDOT, (c) 0.005 M EDOT in ACN solution containing 0.2 M NaClO$_4$ at a scan rate of 100 mV s^{-1}. *j* denotes the current density. E denotes the potential.

The successive cyclic voltammogram (CV) curves of 0.005 M MTP, 0.005 M EDOT and the MTP/EDOT mixture at 1:1 in 0.2 M NaClO$_4$/ACN solution at a potential scan rate of 100 mV s^{-1} are illustrated in Fig. 2. As the CV scan continued, polymer films are formed on the working electrode surface. The increase in the redox wave current densities implies that the amount of conducting polymers deposited on the electrode is increasing [21]. As shown in Fig. 2a, the polymerization of

MTP presents the unsymmetrical redox peaks and the reduction peak potential at 1.24 V, while the corresponding oxidation waves are overlapped with the oxidation waves of the MTP monomer and cannot be observed clearly. The CV curves of EDOT exhibit an anodic peak and a cathodic peak approximately at 0.09 V and -0.61 V, respectively (Fig. 2c). However, the CV curves of the MTP/EDOT mixture at 1:1 show an board anodic peak at around 0.57 V and two well-defined cathodic peak at 0.5 and 1.11 V, respectively (Fig. 2b), which is different from those of MTP and EDOT, indicating the formation of a new copolymer consisting of both MTP and EDOT units [22-24]. In addition, as can be seen from Fig. 2, there is an obvious increase of current density of the MTP/EDOT mixture compared with those of MTP and EDOT, which can also imply the formation of a copolymer [23].
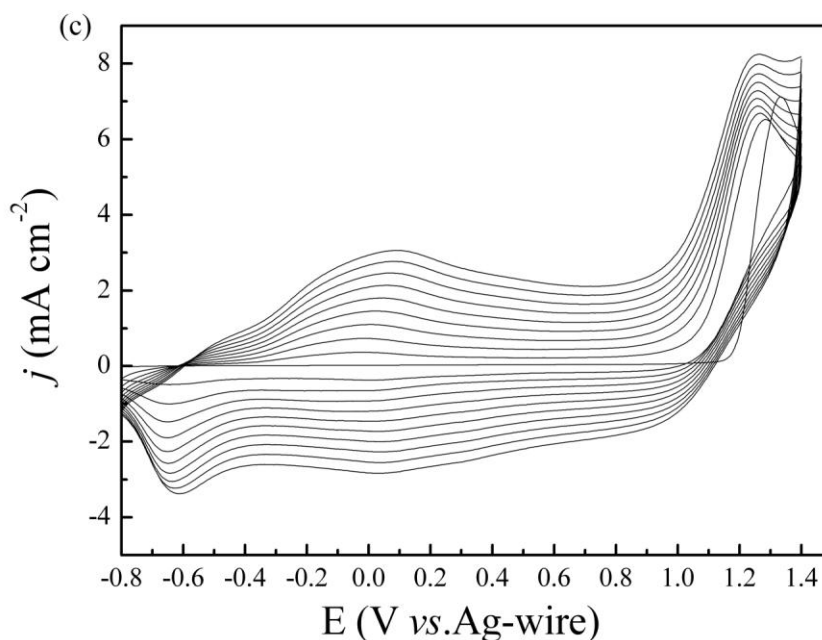
Figure 2. Successive CV curves of (a) 0.005 M MTP, (b) the mixture of 0.005 M MTP and 0.005 M EDOT, (c) 0.005 M EDOT in ACN solution containing 0.2 M NaClO$_4$. Scanning rates: 100 mV s^{-1}. *j* denotes the current density. E denotes the potential.

3.1.2. *Electrochemistry of the P(MTP-co-EDOT) film*

Fig. 3(a) shows the electrochemical behavior of the P(MTP-co-EDOT) film (prepared on platinum wires with the feed ratio of MTP/EDOT at 1:1 by sweeping the potentials from 0 and 1.5 V for three cycles) at different scan rates between 25 and 250 mV s^{-1} in a monomer-free solution of ACN containing 0.2 M NaClO$_4$.
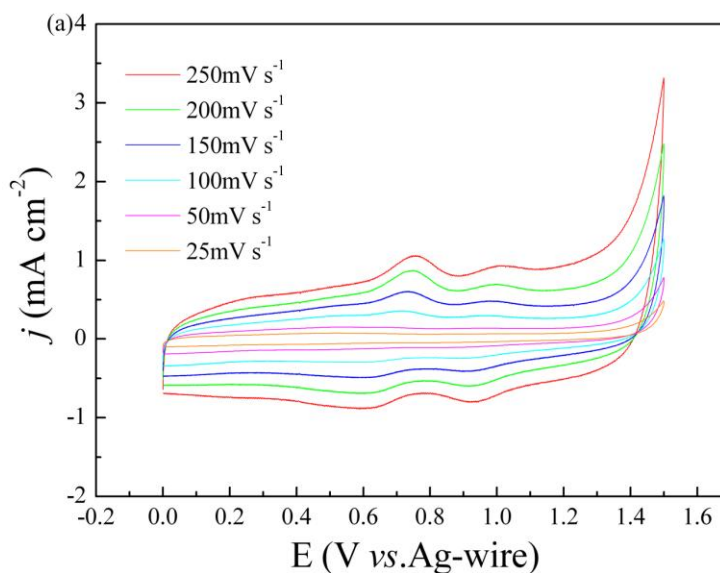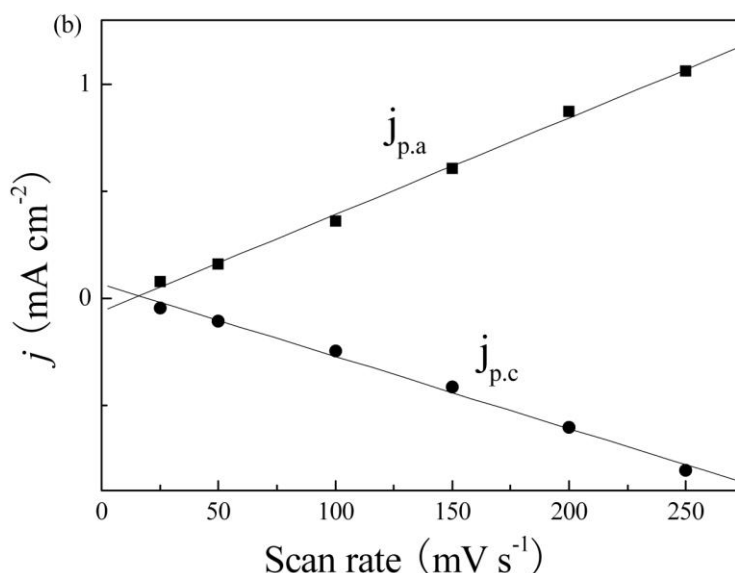
Figure 3. (a) CV curves of the copolymer at different scan rates in the monomer-free solution of ACN containing 0.2 M NaClO$_4$. (b) Scan rate dependence of the anodic and cathodic peak current densities graph. $j_{p.a}$ and $j_{p.c}$ denote the anodic and cathodic peak current densities, respectively.

The copolymer film exhibits two reversible redox processes in Fig. 3(a). The peak current densities (j) are proportional to the potential scan rate (Fig. 3(b)), indicating that the copolymer film is electroactive and adheres well to the electrode [25]. This also demonstrates that the electrochemical processes of the copolymer are reversible and not diffusion limited [26].

3.1.3. Morphology

Scanning electron micrographs (SEM) of polymers provide their clear surface and bulk morphologies, which are closely related to their optical and electrical properties [27].
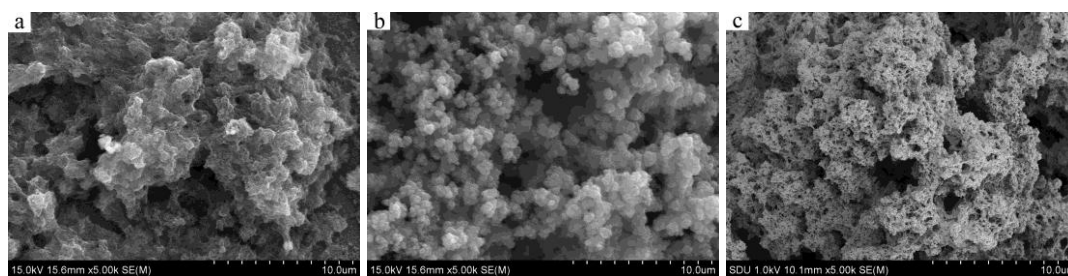

Figure 4. SEM images of (a) MTP, (b) P(MTP-co-EDOT) and (c) PEDOT deposited potentiostatically on ITO electrode.

Fig. 4 gives the SEM images of PMTP, P(MTP-co-EDOT) and PEDOT, which were prepared potentiostatically in the solution of 0.2 M $NaClO_4$/ACN containing relevant monomers on ITO electrodes and dedoped before characterization. As shown in Fig. 4a, PMTP exhibits a coral structure. PEDOT film shows a loose spongy network structure as clusters of floccule (Fig. 4c). However, the copolymer reveals clusters of globules, which is different from the two corresponding homopolymers (Fig. 4b). The difference of morphology between copolymer and homopolymers also confirms the occurrence of copolymerization between MTP and EDOT units.

3.1.4. UV-vis spectra of polymers

Fig. 5 depicts the UV-vis spectra of dedoped (a) PMTP, (b) P(MTP-co-EDOT) and (c) PEDOT deposited on ITO electrode (the active area: 0.9 cm×2.0 cm) with the same polymerization charge ($3.0×10^{-2}$ C). For PMTP film (Fig. 5a), there is an absorption peak at 386 nm due to the π-π* transition. On the other hand, the spectrum of PEDOT film shows the π-π* electron transition peak at about 595 nm (Fig. 5c). While, the maximum absorption peak of the obtained copolymers with 1:1 MTP/EDOT feed ratios shows both the characteristic absorptions of PMTP and PEDOT, which are located at 378 and 568 nm, respectively. However, there is a bit blue shift of the main absorption of copolymer film in contrast to pure PEDOT due to the incorporation unit of MTP, further confirming the occurrence of copolymerization [28]. Fine tuning in the band gap is achieved by tailoring the co-monomer feed ratio of copolymerization.
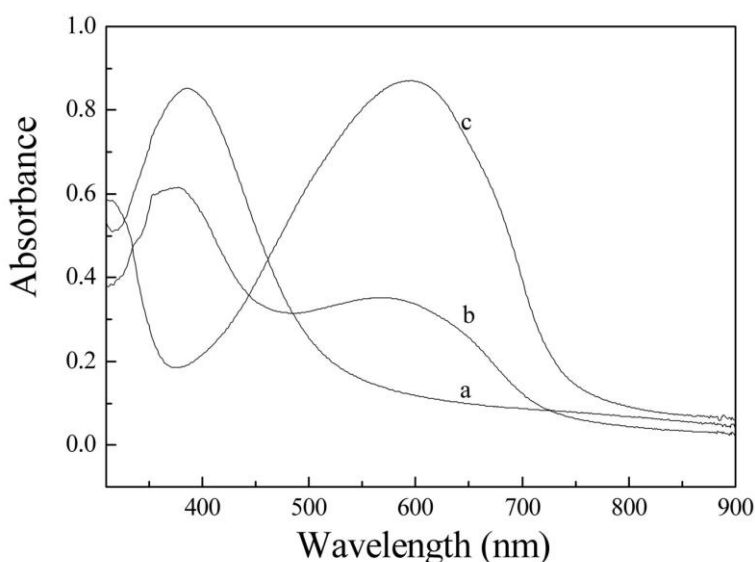

Figure 5. UV-vis spectra of dedoped (a) MTP, (b) the copolymers prepared with the feed ratio of MTP/EDOT at 1:1 and (c) PEDOT deposited on ITO at the neutral state.

Besides, the optical band gap (E_g) of polymer was deduced from the absorption band edges (λ_{onset}) ($E_g = 1240/\lambda_{onset}$). The λ_{onset} of PMTP, P(MTP-co-EDOT) and PEDOT are at 630 nm, 725 nm

and 760 nm, respectively. The E_g of the P(MTP-co-EDOT) was calculated as 1.71 eV, which was lower than that of PMTP (1.96 eV) and higher than that of PEDOT (1.63 eV). The effect of copolymerization between MTP and EDOT leads to an obvious decrease in the E_g comparing with that of PMTP, which implies that the introduction of EDOT units into PMTP can tune the conjugation of the copolymer.

Table 1 summarizes the onset oxidation potential (E_{onset}), maximum absorption wavelength (λ_{max}), low energy absorption edges (λ_{onset}), HOMO and LUMO energy levels and the optical band gaps (E_g) values of PMTP, P(MTP-co-EDOT) and PEDOT. HOMO energy levels of them are calculated by using the formula $E_{HOMO} = -e(E_{onset} + 4.43)$ (vs. SCE) and LUMO energy levels (E_{LUMO}) of them are calculated by the subtraction of the optical band gap (E_g) from the HOMO levels [29].

Table 1. The onset oxidation potential (E_{onset}), maximum absorption wavelength (λ_{max}), low energy absorption edges (λ_{onset}), HOMO and LUMO energy levels and optical band gap (E_g) values of PMTP, PEDOT, and the copolymers (prepared with the feed ratio of MTP/EDOT at 1:1).

Compounds	E_{onset}, vs.(Ag-wire) (V)	λ_{max} (nm)/ λonset (nm)	E_g[a] (eV)	HOMO (eV)	LUMO[b] (eV)
PMTP	0.33	386/630	1.96	-4.76	-2.80
P(MTP-co-EDOT)	0.02	378/725	1.71	-4.45	-2.74
PEDOT	-0.62	595/760	1.63	-3.81	-2.18

[a] Calculated from the low energy absorption edges (λ_{onset}).

[b] Calculated by the subtraction of the optical band gap (E_g) from the HOMO level.

3.2. Electrochromic properties of P(MTP-co-EDOT) film

3.2.1 Spectroelectrochemical properties of P(MTP-co-EDOT) film

Spectroelectrochemistry is a useful method for studying the changes in the absorption spectra and the information about the electronic structures of conjugated polymers as a function of the applied potential difference [30]. The P(MTP-co-EDOT) film coated ITO electrode was switched between neutral (-0.6 V) and doped (1.5 V) states in monomer-free 0.2 M $NaClO_4$/ACN solution in order to obtain the in situ UV-vis spectra (Fig. 6). At the neutral state, the copolymer film exhibits an absorption band at 563 nm due to the π-π* transition. The intensity of the P(MTP-co-EDOT) π-π* electron transition absorption decreases while a charge carrier absorption band located at around 775 nm increase dramatically upon oxidation. The appearance of charge carrier bands can be attributed to the evolution of polaron and bipolaron bands.
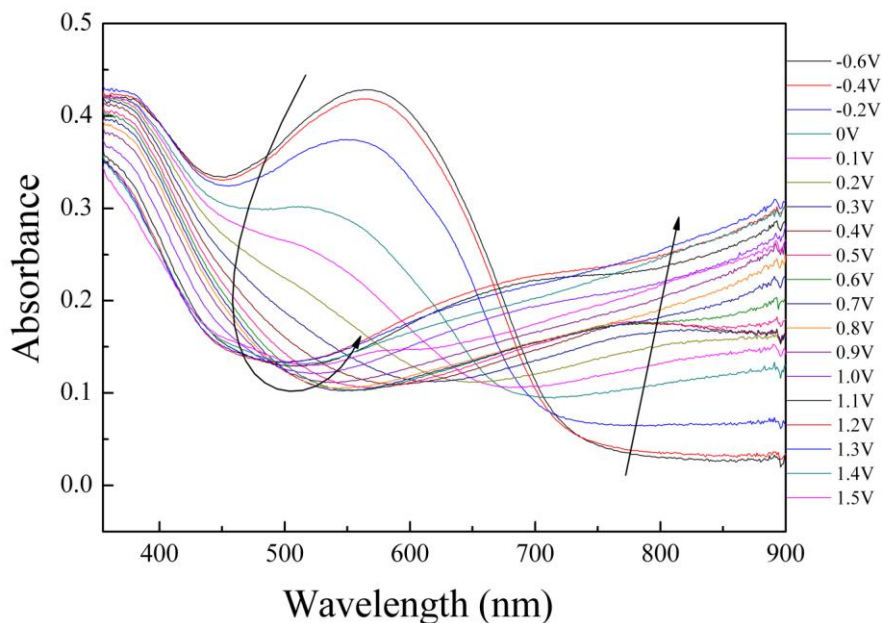
Figure 6. Spectroelectrochemical spectra of P(MTP-co-EDOT) with applied potentials between -0.6V and 1.5 V in monomer-free ACN solution containing 0.2 M NaClO$_4$.

It was interesting to find that the P(MTP-co-EDOT) film showed a multicolor electrochromism. In order to study the range of colors, a wide interval of potentials (-0.6 V to 1.5 V) is applied on the as-prepared P(MTP-co-EDOT) films. As can be seen from Fig. 7, P(MTP-co-EDOT) film shows four different colors in neutral and oxidized states. The purple color of the film at neutral state (-0.6 V) turns into brown color (0.1 V) and grass green (0.7 V) at intermedia doped state, and then it becomes dusty blue color at full doped state (1.5 V). This multicolor property possesses significant potential applications in smart windows or displays and so on [31].
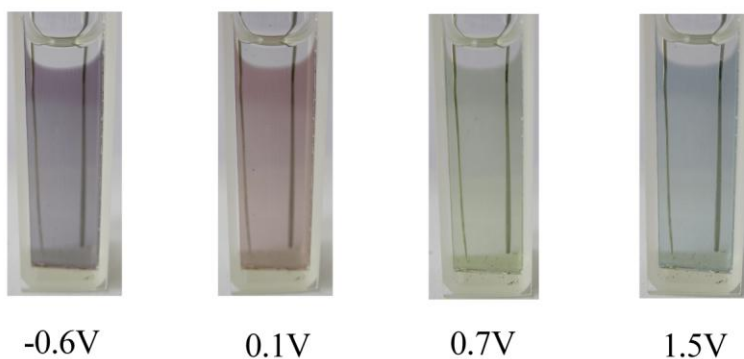

Figure 7. Colors of the P(MTP-co-EDOT) film at different applied potentials in ACN solution containing 0.2 M NaClO$_4$.

3.2.2 Electrochromic switching of P(MTP-co-EDOT) film in solution

It is important that polymers can switch rapidly and exhibit a noteworthy color change for electrochromic applications [32]. For this purpose, double potential step chronoamperometry technique was used to investigate the switching ability of P(MTP-co-EDOT) film between its neutral and full doped state (Fig. 8) [33]. The dynamic electrochromic experiment for P(MTP-co-EDOT) film was carried out at 570 nm. The potential was interchanged between -0.4 V (the neutral state) and 1.1 V (the oxidized state) at regular intervals of 3 s. One important characteristic of electrochromic materials is the optical contrast ($\Delta T\%$), which can be defined as the transmittance difference between the redox states. The $\Delta T\%$ of the P(MTP-co-EDOT) was calculated to be 15.31 % at 570 nm, as shown in Fig. 8.

The coloration efficiency (CE) is also an important characteristic for the electrochromic materials. CE can be calculated by using the equations and given below [34]:

$$\Delta OD = \log\left(\frac{T_b}{T_c}\right) \quad \text{and} \quad \eta = \frac{\Delta OD}{\Delta Q}$$

where T_b and T_c are the transmittances before and after coloration, respectively. ΔOD is the change of the optical density, which is proportional to the amount of created color centers. η denotes the coloration efficiency (CE). ΔQ is the amount of injected charge per unit sample area. CE of P(MTP-co-EDOT) film was measured as $61.78 \text{cm}^2 \text{ C}^{-1}$ (at 570 nm) , which had reasonable coloration efficiency.
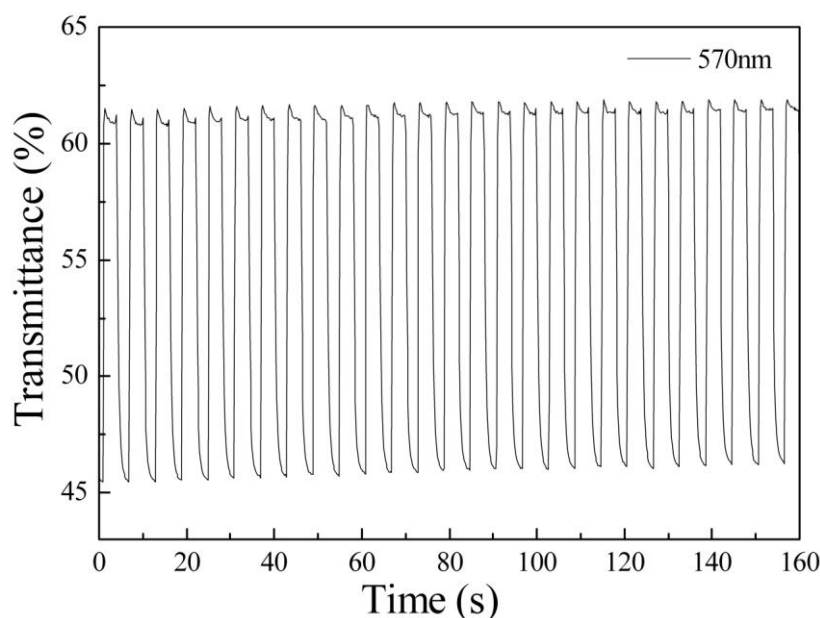

Figure 8. Electrochromic switching for P(MTP-co-EDOT) film under an applied square voltage signal between -0.4 V and 1.10 V with a residence time of 3 s at 570 nm.

Response time, one of the most important characteristics of electrochromic materials, is the time needed to perform a switching between the neutral state and oxidized state of the materials [13].

The response required to attain 95% of total transmittance difference was found to be 0.35 s from the reduced to the oxidized state and 1.28 s from the oxidized to the reduced state. Based on the discussion, the distinct optical contrast, the satisfactory coloration efficiency and switching property make P(MTP-co-EDOT) a promising electrochromic material.

3.3. Spectroelectrochemistry of electrochromic devices (ECDs)

3.3.1 Spectroelectrochemical properties of ECD

A dual type ECD consisting of P(MTP-co-EDOT) and PEDOT constructed and its spectroelectrochemical behaviors were also studied. Before composing the ECD, the anodic polymer film (P(MTP-co-EDOT)) was fully reduced and the cathodic polymer film (PEDOT) was fully oxidized. The P(MTP-co-EDOT)/PEDOT device was switched between -0.8 and 1.5 V. The spectroelectrochemical results are shown in Fig. 9. At -0.8 V, the P(MTP-co-EDOT) layer was in its neutral state and PEDOT was in oxidized state and the device color was dark green. Thus, there was maximum absorption at around 410 nm due to π-π* transition of the electrochromic layer of P(MTP-co-EDOT). As the applied potential increased, the P(MTP-co-EDOT) layer started to be oxidized and the intensity of the peak due to the π-π* transition decreased, while PEDOT layer was reduced and evolution of a new intense absorption at around 615 nm (π-π* transition of PEDOT itself), and the dominated color of the device was slategray at 1.5V.
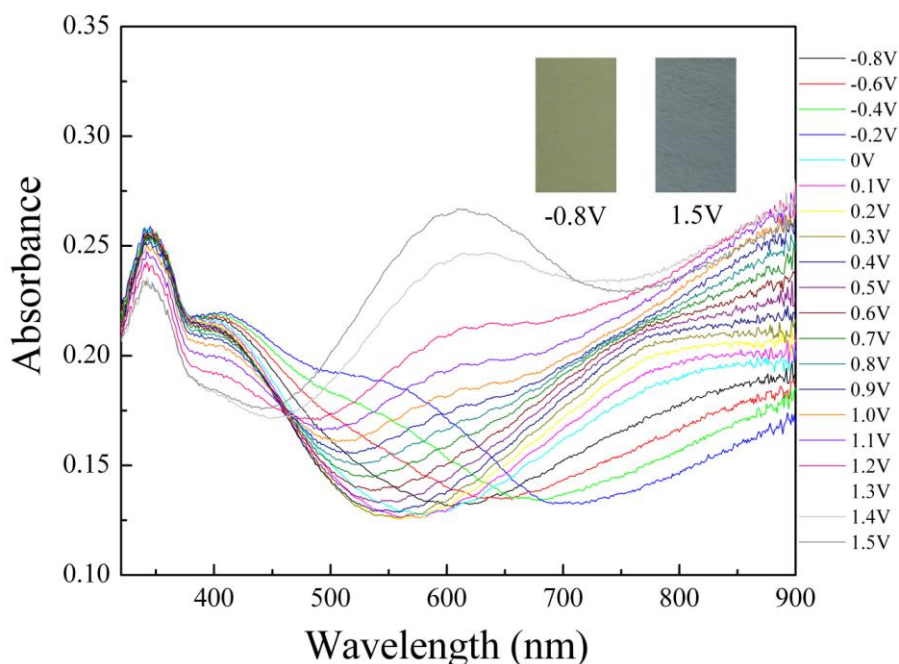

Figure 9. Spectroelectrochemical spectra of the P(MTP-co-EDOT)/PEDOT device at various applied potentials between -0.8 and 1.5 V.

3.3.2. Switching of ECD

Kinetic studies were also done to test the percent transmittance changes and the response time of P(MTP-co-EDOT)/PEDOT ECD. Under a potential input of -0.8V and 1.4 V at regular intervals of 3 s, the optical response at 690 nm was illustrated in Fig. 10. The response time is found to be 0.9 s at 95% of the maximum transmittance difference from the neutral state to oxidized state and 0.51 s from the oxidized state to the neutral state, and optical contrast ($\Delta T\%$) is calculated to be 14.81%. The CE of the P(MTP-co-EDOT)/PEDOT device (the active of area is 1.8 cm×2.0 cm) is calculated to be 242.6 cm^2 C^{-1} at 690 nm.
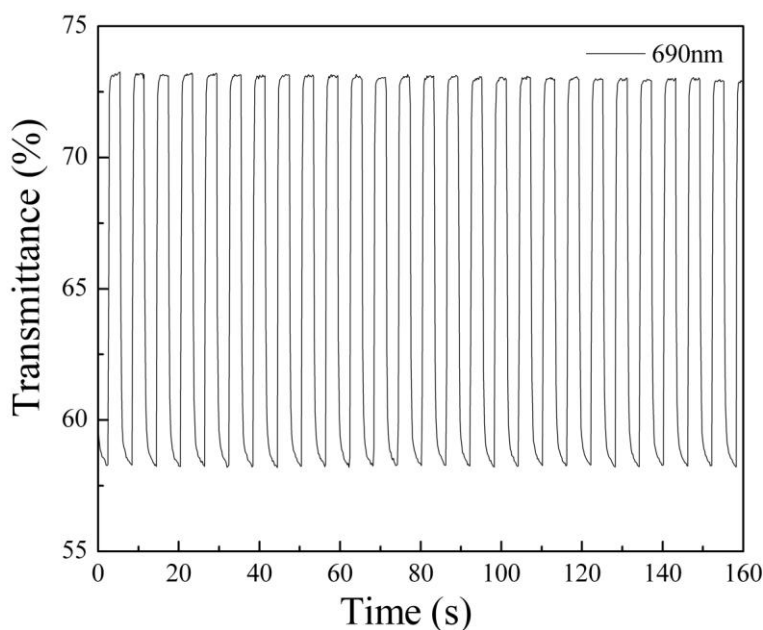

Figure 10. Electrochromic switching, optical transmittance change monitored at 690 nm for P(MTP-co-EDOT)/PEDOT device between -0.8 V and 1.4 V with a residence time of 3 s.

3.3.3 Open circuit memory of ECD

The optical memory in the electrochromic devices is an important parameter because it is directly related to its application and energy consumption during the use of ECDs [35]. The optical spectrum for P(MTP-co-EDOT)/PEDOT device was monitored at 690 nm as a function of time at -0.8 V and 1.4 V by applying the potential for 1 s for each 200 s time interval. As shown in Fig. 11, light yellow colored state device showed a true permanent memory effect since there was almost no transmittance change under applied potential or open circuit conditions. In blue colored state device was rather less stable in terms of color persistence, however this matter can be overcome by application of current pulses to freshen the fully colored states.
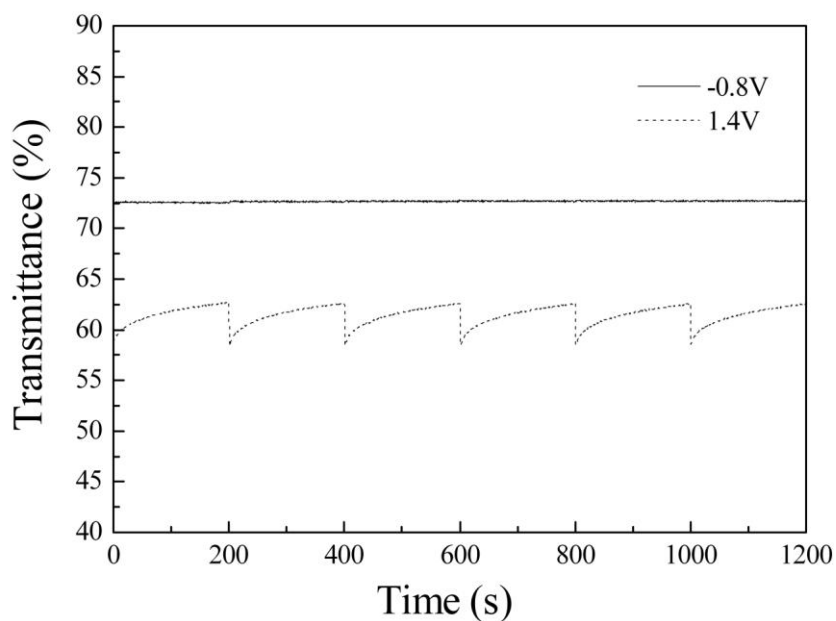
Figure 11. Open circuit stability of the P(MTP-co-EDOT)/PEDOT device monitored at 630 nm.

3.3.4 Stability of the ECD

The stability of the devices toward multiple redox switching usually limits the utility of electrochromic materials in ECD applications. Therefore, redox stability is another important parameter for ECD [36].
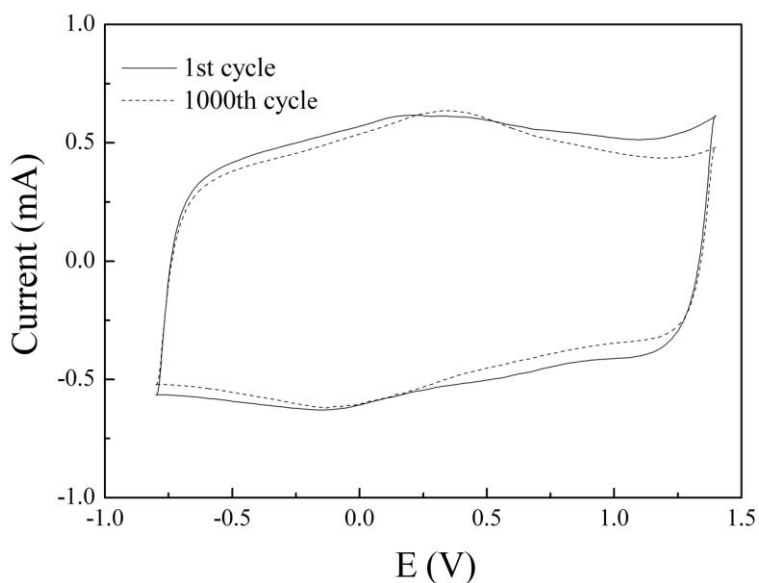

Figure 12. Cyclic voltammogram of P(MTP-co-EDOT)/PEDOT device as a function of repeated with a scan rate of 500 mV/s.

For this reason, the P(MTP-co-EDOT)/PEDOT device was tested by cyclic voltammetry of the applied potential between -0.8 V and 1.4 V with 500 mV s^{-1} to evaluate the stability of the device (Fig. 12). After 1000 cycles, 93.11% of its electroactivity is retained. These results show that this device has good redox stability.

4. CONCLUSION

A novel low band gap copolymer based on MTP and EDOT was successfully synthesized via electrocopolymerization. Cyclic voltammetry (CV), UV-vis spectroscopy and scanning electron microscopy (SEM) confirmed that the resultant polymer is a copolymer rather than a blend or a composite of the respective homopolymers. The P(MTP-co-EDOT) film had exhibited excellent multicolor electrochromism (purple, brown, grass green and dusty blue) under various potentials. The low energy absorption edge of the P(MTP-co-EDOT) was at 725 nm corresponding to a band gap of 1.71 eV. It showed that copolymerization with EDOT decreased the band gap (E_g). The dual-type electrochromic device (ECD) based on P(MTP-co-EDOT) and PEDOT is also constructed and characterized. Electrochromic switching study results show that optical contrast ($\Delta T\%$) and response time are 14.81% and 0.51 s at 690 nm, respectively. The coloration efficiency (CE) of the device is calculated to be 242.6 cm^2 C^{-1}. In addition, the device had good redox stability. For those reasons, it can be considered as a promising candidate for commercial applications.

References

1. H. Seol, H. Jeong, S. Jeon, *J. Electroanal. Chem.* 636 (2009) 107.
2. S. Gunes, H. Neugebauer and N. S. Sariciftci, *Chem. Rev.* 107 (2007) 1324.
3. H. Zhang, J. Zhao, H. Liu, H. Wang, R. Liu, J. Liu, *Int. J. Electrochem. Sci.* 5 (2010) 295.
4. A. Azens, C.G. Granqvist, *J. Solid State Electrochem.* 7 (2003) 64.
5. J.H. Kang, Z.C. Xu, S.M. Paek, F. Wang, S.J. Hwang, J. Yoon, J.H. Choy, *Chem. Asian J.* 6 (2011) 2123.
6. M. Ak, E. Şahmetlioğlu, L. Toppare, *J. Electroanal. Chem.* 621 (2008) 55.
7. Trakool Kumchoo, Vinich Promarak, T aweesak Sudyoadsuk, Mongkol Sukwattanasinitt, Paitoon Rashatasakhon, *Chem. Asian J.* 5 (2010) 2162.
8. L.Y. Xu, J.S. Zhao, C.S. Cui, R.M. Liu, J.F. Liu, H.S. Wang, *Electrochim. Acta.* 56 (2011) 2815.
9. M. Sendur, A. Balan, D. Baran, B. Karabay, L. Toppare, *Org. Electron.* 11 (2010) 1877.
10. L.B. Groenendal, G. Zotti, P.H. Aubert, S.M. Waybright, J.R. Reynolds, *Adv. Mater.* 15 (2003) 855.
11. B. Wang, J.S. Zhao, C.S. Cui, R.M. Liu, J.F. Liu, H.S. Wang, H.T. Liu, *Electrochim. Acta.* 56 (2011) 4819.
12. Serhat Varis, Metin Ak, Idris M. Akhmedov, Cihangir Tanyeli, Levent Toppare, *J. Electroanal. Chem.* 603 (2007) 8.

13. B. Yigitsoy, S. Varis, C. Tanyeli, I.M. Akhmedov, L. Toppare, *Electrochim. Acta.* 52 (2007) 6561.
14. C. C.Chang, L. J.Her, J. L.Hong, *Electrochim. Acta*. 50 (2005) 4461.
15. X.F. Cheng, J.S. Zhao, C.S. Cui, Y.Z. Fu, X.X. Zhang, *J. Electroanal. Chem.* 24 (2012) 677.
16. X.B. Wan, W. Zhang, S. Jin, G. Xue, Q.D. You, B. Che, *J. Electroanal. Chem.* 470 (1999) 23.
17. G.M. Nie, L.Y. Qu, Y. Zhang, J.K. Xu, S.S. Zhang, *J. Appl. Polym. Sci.* 109 (2008) 373.
18. P. Novak, W. Vielstich, *J. Electroanal. Chem.* 300 (1991) 99.
19. C.L. Gaupp, J.R. Reynolds, *Macromolecules.* 36 (2003) 6305.
20. V. Seshadri, L.D. Wu, G.A. Sotzing, *Langmuir.* 19 (2003) 9479.
21. C. Zhang, Y. Xu, N. Wang, Y. Xu, W. Xiang, M. Ouyang, C. Ma, *Electrochim. Acta.* 55 (2009) 13.
22. C. Kvarnstrom, H. Kulovaara, P. Damlin, T. Vuorinen, H. Lemmetyinen, *A. Ivaska, Synth. Met.* 149 (2005) 39.
23. G.M. Nie, L.Y. Qu, J.K. Xu, S.S. Zhang, *Electrochim. Acta.* 53 (2008) 8351.
24. S. Demoustier-Champagne, J.R. Reynolds, *M. Pomerantz, Chem. Mater.* 7 (1995) 277.
25. G. W. Lu, G. Q. Shi, *J. Electroanal. Chem.* 586 (2006) 154.
26. M. Ak, M.S. Ak, G. Kurtay, M. Güllü, L. Toppare, *Solid State Sci.* 12 (2010) 1199.
27. H.T. Liu, Y.Z. Li, J.K. Xu , Z.G. Le, M.B. Luo, B.S. Wang, S.Z. Pu, L. Shen, *Eur. Polym. J.* 44 (2008) 171.
28. L.Y. Xu, J.S. Zhao, R.M. Liu, H.T. Liu, J.F. Liu, H.S. Wang, *Electrochim. Acta.* 55 (2010) 8855.
29. D.M. de Leeuw, M.M.J. Simenon, A.R. Brown, R.E.F. Einerhand, *Synth. Met.* 87 (1997) 53.
30. J. Hwang, J.I. Son, Y.-B. Shim, *Sol. Energy Mater. Sol. Cells.* 94 (2010) 1286.
31. M. Ouyang, G.H. Wang, C. Zhang, *Electrochim. Acta.* 56 (2011) 4645.
32. E. Yildiz, P. Camurlu, C. Tanyeli, I. Akhmedov, L. Toppare, *J. Electroanal. Chem.* 612 (2008) 247.
33. E. Sefer, F.B. Koyuncu, E. Oguzhan, S. Koyuncu, *J. Polym. Sci.: Part A: Polym. Chem.* 48 (2010) 4419.
34. S. J. Yoo, J. H. Cho, J. W. Lim, S. H. Park, J. Jang, Y.-E. Sung, *Electrochem. Commun.* 12 (2010) 164.
35. W.A. Gazotti, J.R.G. Casalbore-Micelli, A. Geri, M.A. De-Paoli, *Adv. Mater.* 10 (1998) 60.
36. C. Bechinger, M. S. Burdis, J. G. Zhang, *Solid State Commun.* 101 (1997) 753.
37. W.Y. Yu, J. Chen, Y.L. Fu, J.K. Xu, G.M. Nie, *J. Electroanal. Chem.*700 (2013) 17.